Applied Physics A (2021) 127:538
https://doi.org/10.1007/s00339-021-04699-z

Applied Physics A
Materials Science & Processing

Green synthesized $MgFe_2O_4$ ferrites nanoparticles for biomedical applications

R. Shunmuga Priya[1] · E. Ranjith Kumar[2] · A. Balamurugan[3] · Ch. Srinivas[4]

Received: 3 April 2021 / Accepted: 13 June 2021 / Published online: 19 June 2021

Abstract
In this present work, we adopted a modified lemon juice-involved combustion method to prepare $MgFe_2O_4$ nanoparticles (MgFNPs). The prepared MgFNPs are subjected to annealing treatment at different temperatures. The synthesized and annealed MgFNPs have been studied using various techniques to analyze their structural, morphological and biomedical activities. X-ray diffraction (XRD), scanning electron microscopy (SEM) and transmission electron microscopy (TEM) were used to examine the crystallite nature, shape and particles size of MgFNPs. The crystallite sizes are found in the range 10.1 nm to 32.7 nm. For various annealing temperatures, the effects of annealing treatment on structural parameters are also investigated. The spherical-shaped nanoparticle was recorded through SEM and TEM. The average size of the particles was determined from TEM micrographs using Histogram plot is 36.7 nm which is well matched with the crystallite size calculated from XRD profile. The antimicrobial activities of MgFNPs were tested against Gram-positive (B.subtilis) and Gram-negative (E.coli) bacteria by plate counting method. MgFNPs nanoparticles show strong antibacterial activity toward Gram-negative than Gram-positive bacteria.

Keywords Nanoparticles · Lemon-assisted combustion synthesis · Microstructure · TEM · Biomedical applications

1 Introduction

In recent days, magnetic nanoparticles have been widely synthesized for different technological applications like microwave units, computer memory chips and high-density storage media. MgFNPs, a type of magnetic nanoparticle, are a promising material for catalysts, gas sensors, humidity sensors and inorganic pigment, among other applications. The synthesis of fine powders of high purity is indispensable for these applications. Nowadays, numerous chemical methods have been used to prepare MgFNPs, including sol–gel combustion, polymeric method, microwave combustion, microemulsion, co-precipitation, hydrothermal methods and reverse micelle [1, 2], etc. Nowadays, green synthesis methods are widely used to prepare different types of nanoparticles for various applications [3–5]. Druc et al. [6] prepared Mg-ferrite nanoparticles using sol–gel auto-combustion route. A variety of fuels like glycine, citric acid, urea, tartaric acid, cellulose and hexamethylenetetramine were used to prepare Mg-ferrite nanoparticles. A single-phase MgFNPs have been prepared using glycine, citric acid and tartaric acid. The secondary impurity phase has been identified for the samples prepared by urea, cellulose and hexamethylenetetramine, even at higher-order annealing treatment. However, the pure single-phase MgFNPs obtained by Nakagomi et al. [7] and Franco et al. [8] using urea as a fuel. Using citrate gel route many researchers synthesized MgFNPs without any secondary impurity phases [9]. Pure single-phase nanoparticles were successfully obtained by glycine-based synthesis of MgFNPs by the auto-combustion process [10]. Generally, in the synthesis of MgFNPs, α-Fe_2O_3 exists as an impurity phase. It is also worth finding a new route to obtain single-phase MgFNPs. Ngozi Madubuonu et.al [11] reported the Psidium guajava aqueous extract used green synthesis

✉ E. Ranjith Kumar
ranjueaswar@gmail.com

[1] Department of Physics, Emerald Heights College for Women, Ooty, The Nilgiris 643006, Tamil Nadu, India

[2] Department of Physics, KPR Institute of Technology & Engineering, Coimbatore 641 407, Tamil Nadu, India

[3] Department of Physics, Government Arts and Science College, Avinashi 641654, Tamil Nadu, India

[4] Nanomaterials and Nanomagnetism Research Laboratory, Department of Physics, Sasi Institute of Technology & Engineering, Tadepalligudem 534101, Andhra Pradesh, India

of Fe oxide nanoparticles and their performance against antibacterial activities. Samson O. Aisida et.al [5] reported structural, optical, morphological and magnetic properties of green synthesized $ZnFe_2O_4$ nanoparticles for moderate hyperthermia applications. The main aim of this work is to synthesize MgFNPs using the lemon juice-assisted combustion method. The lemon juice was used successfully in order to synthesize fine and pure nanophase MgFNPs. The crystallite size, morphology and antimicrobial activities of MgFNPs have been examined.

2 Experimental methods

2.1 Synthesis

Lemon juice-aided combustion was used to make MgFNPs. To make MgFNPs nanoparticles, raw materials such as analytical grade $Mg(NO3)_26H2O$ and Fe $(NO3)_39H2O$ were used. These materials were taken at high molar concentrations to keep the stoichiometric Mg/Fe ratio of 1:2. 50 mL lemon juice is added to the precursor solutions to act as a chelating agent (natural citric acid). This solution mixture was thoroughly blended for 1 h. The mixed solution was further stirred with a magnetic stirrer at 100 °C until the necessary final ferrite powder was obtained. In an agate mortar, the ferrite powder was milled into a fine powder and a portion of it was heat treated in the air at 600 °C and 900 °C. For our convenience, the samples were coded M-1 (as-prepared), M-2 (annealed at 600 °C) and M-3(annealed at 900 °C). The structural, microstructural and antimicrobial activities of these samples were all examined.

2.2 Techniques of characterization

Phillip's X'pert-PRO X-ray powder diffractometer with CuK al1 (= 1.5406) radiation was used to record XRD patterns.

A JEOL JSM-6610L scanning electron microscope with EDX was used to capture SEM images and EDX spectra. The antibacterial property of MFNPs was investigated using the plate count method with two bacterial species, E. coli (ATCC 14,948) and B. subtilis (ATCC 11,774).

3 Results and discussion

XRD patterns of sintered Mg-nanoferrite and as-prepared Mg-nanoferrite are shown in Fig.1. The formation of Mg-ferrite with cubic spinel structure is confirmed by the observed diffraction peaks. The diffraction spikes (220), (311), (400), (422), (511) and (440) are well-suited to the fd3 m space group, which corresponds to JCPDS card no. 01-071-1232. The sharpness of a diffraction peak is slowly

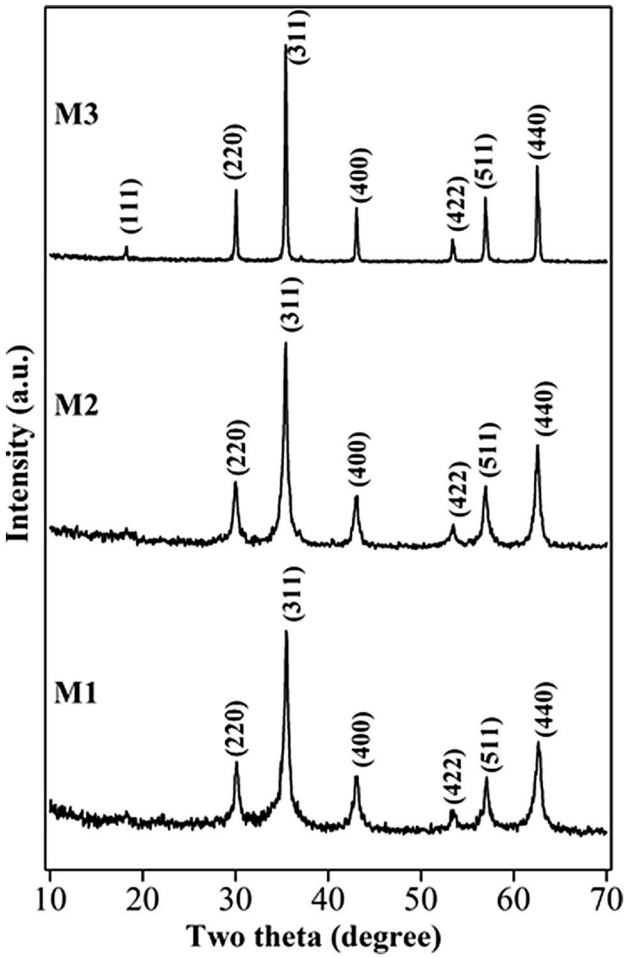

Fig. 1 XRD pattern of $MgFe_2O_4$ nanoparticles

rising, but expansion occurs near the base of the peaks. It is because ferrite nanoparticles of different sizes coexist. As previously mentioned, the formation of the Mg-ferrite spinel phase is highly dependent on preparation methods, sintering temperature, fuel molar fractions and other variables. Aslibeiki et al. discovered secondary phases of alpha-Fe_2O_3 in a $MgFe_2O_4$ sample sintered at 600 °C [12]. Prasad et al. [13] looked into the function of precursors in the formation of different spinel ferrites. A thorough examination of secondary phase formation in various spinel ferrites has been reported. They proposed that the local oxygen condition and heat treatment influence the formation of secondary phases in spinel ferrite systems. They argue that when sintering at a higher temperature, the thermal energy is adequate to remove the internal oxygen environment that causes ferrite decomposition, while when sintering at a lower temperature, the thermal energy is insufficient. Structural parameters such as crystallite size (*t*) and lattice constant (a) were calculated using the formulas $t = (0.9\ \lambda) / (\beta \cos \theta)$ and $a^2 = d^2\ (h^2 + k^2 + l^2)$. In addition, the experimental lattice parameter

decreases monotonically from 8.403 to 8.397 as the sintering temperature rises. The rearrangement of cations between the spinel structure sites A- and B- is clearly visible. The crystallite sizes of the samples range from 10.1 to 32.9 nm on average. The scale of the crystallite expands as the sintering temperature rises. By increasing grain boundary energy, the sintering process promotes crystallization.

The analysis of how objects appear is known as morphology. The morphology and elemental composition of a sample annealed at 900 °C (M3) are shown in Fig. 2(a, b and c). The existence of micro-pictures makes it difficult to determine the form of ferrite nanoparticles. Powerful magnetic interactions, on the other hands, clearly show the formation of nanosized ferrite particles coalescing into clusters of various sizes. The EDX spectra are shown in Fig. 2b. The achievement of the ferrite process was revealed under-considered stoichiometry when the elemental ratios of Mg/Fe and Fe/O were close to 0.5. Other elemental spikes and oxygen depletion have not been detected in spectra. The MgFe2O4 nanoparticles in sample M3 are almost spherical in shape, with an average particle size of 36.7 nm, according to TEM images (Fig. 2c). The SAED pattern clearly established the polycrystalline nature of the sample.

The antibacterial activity of MgFe2O4 nanoparticles was calculated using the plate counting method against Gram-positive (B.subtilis) and Gram-negative (E.coli) bacteria. The pathogens on the different plates were inoculated in the culture media with Gram-positive and Gram-negative pathogens. Then, on the appropriate plates, the synthesized samples of MgFe2O4 nanoparticles at various concentrations (0.1, 1, 10, 25 and 50 Mg/L) were mounted. The percent of toxicity around the samples was assessed after 24 h. The biocidal activity of MgFe2O4 nanoparticles at various temperatures (as-burnt, 600 °C and 900 °C) is shown in Fig. 3. With increasing sample concentrations, MgFe2O4 nanoparticles' antibacterial activity increases. At 50 mg/L, toxicity was observed against Gram-negative (E.coli) and Gram-positive (B.subtilis) bacteria in M1, M2 and M3, with 78 percent and 58 percent, 69 percent and 35 percent and 44 percent and 33 percent, respectively. The antibacterial activity of the MgFe2O4 nanoparticles decreases as the calcination temperature rises from 600 to 900 °C. As the temperature rises, so does the particle size. Since the particle size is smaller at lower temperatures, the killing effect is greater. Since particle size grows larger as temperature rises, the killing effect decreases. As a consequence, as the temperature rises, the particle size rises with it. Table 1 shows the percent of toxicity that is inversely proportional to temperature. When M1, M2 and M3 are compared, M1 has the most potent toxic effect against bacterial pathogens. It is likely due to the size effect. Based on Gram-positive and Gram-negative

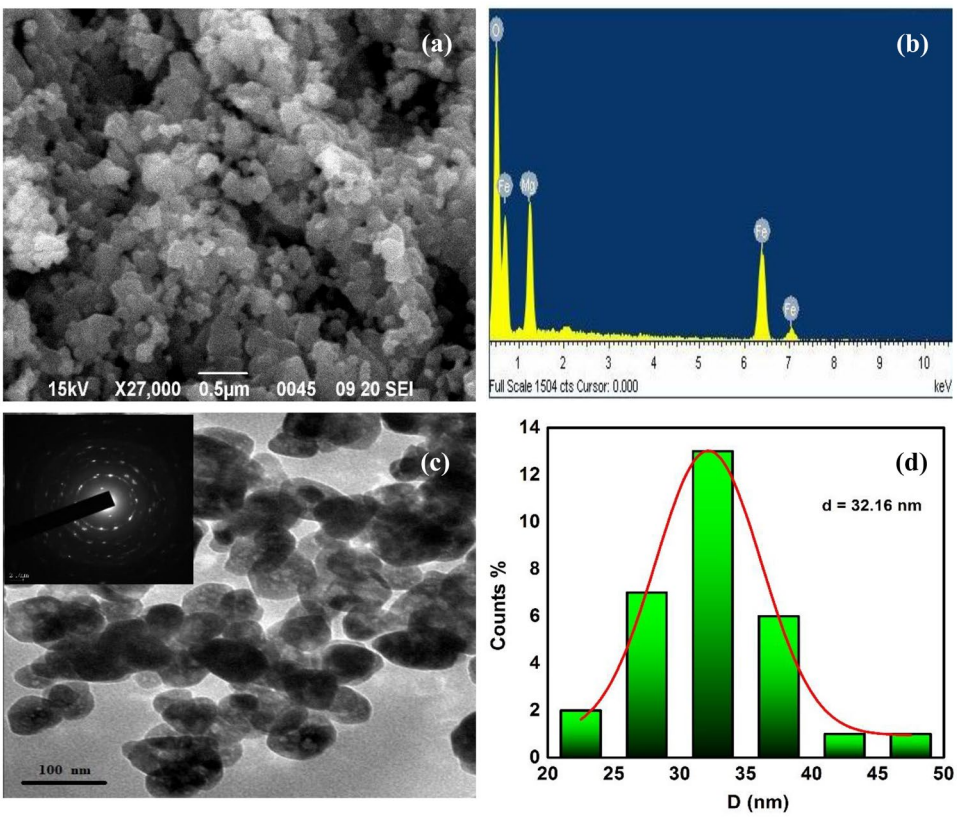

Fig. 2 SEM, EDX and TEM images of $MgFe_2O_4$ nanoparticles

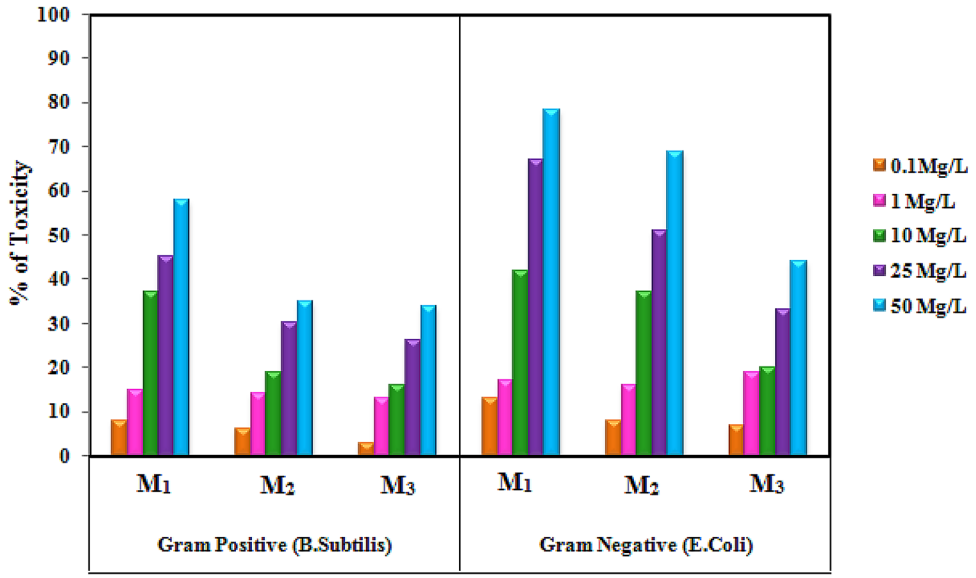

Fig. 3 Antibacterial activity of $MgFe_2O_4$ nanoparticles

Table 1 Antibacterial activities of $MgFe_2O_4$ nanoparticles

Concentrations Mg/L	% of Toxicity					
	Gram-positive (B.subtilis)			Gram-negative (E.coli)		
	M_1	M_2	M_3	M_1	M_2	M_3
0.1	7.8	6	3	13	8	7
1	15	14	13	17	16	19
10	37	19	16	42	37	20
25	45	30	26	67	51	33
50	58	35	34	78	69	44

bacteria, it has been discovered that MgFe2O4 nanoparticles have greater antibacterial activity against Gram-negative bacteria than Gram-positive bacteria, which may be due to variations in cell structure and peptide glycan cell wall thickness [14].

4 Conclusions

Lemon juice was used to make pure single-phase MgFe2O4 nanoferrites. The crystallite sizes of the samples were found to be between 10.1 and 32.7 nm. The samples' lattice constant (a) decreases as the annealing temperature rises. The spherical nanoparticle is photographed under a microscope and the measured size matches that of XRD. Gram-positive (B.subtilis) and Gram-negative (E.coli) bacteria were used to test the antibacterial activity of MgFe2O4 nanoparticles. Gram-negative bacteria are more resistant to $MgFe_2O_4$ nanoparticles than Gram-positive bacteria.

References

1. A. Goldman, *Modern Ferrite Technology*, 2nd edn. (Springer Science Business Media Inc., New York, 2006)
2. Yuxiang Feng, Shanshan Li, Yali Zheng, Ziwei Yi, Yanyan He, Yebin Xu, J. alloy. comp, 699 (2017) 521–525.
3. S.O. Aisida, K. Ugwu, A.C. Nwanya, A.K.H. Bashir, N. Uba Nwankwo, I. Ahmed, F.I. Ezema, Biosynthesis of silver oxide nanoparticles using leave extract of Telfairia Occidentalis and its antibacterial activity. Mater Today: Proceedings. **36**, 208–213 (2021)
4. S.O. Aisida, K. Ugwu, P.A. Akpa, A.C. Nwanya, U. Nwankwo, A.K.H. Bashir et al., Synthesis and characterization of iron oxide nanoparticles capped with Moringa Oleifera: The mechanisms of formation effects on the optical, structural, magnetic and morphological properties. Mater Today: Proceedings. **36**, 214–218 (2021)
5. S.O. Aisida, A. Ali, O.E. Oyewande et al., Biogenic synthesis enhanced structural, morphological, magnetic and optical properties of zinc ferrite nanoparticles for moderate hyperthermia applications. J Nanopart Res **23**, 47 (2021)
6. A. Druc, A. Dumitrescu, A. Borhan, V. Nica, A. Iordan, M. Palamaru, Cent. Eur. J. Chem. **11**, 1330–1342 (2013)
7. F. Nakagomi, S.W. Da Silva, V.K. Garg, A.C. Oliveira, P.C. Morais, A. Franco Jr., Solid State Chem. **182**, 2423–2429 (2009)

8. A. Franco Jr., T.E. Pereira Alves, E.C. de Oliveira Lima, E. da Silva Nunes, V. Zapf, Appl. Phys. A 94 (2009) 131–137.
9. J.Y. Patil, I.S. Mulla, S.S. Suryavanshi, Mater. Res. Bull. **48**, 778–784 (2013)
10. N.M. Deraz, A. Alarifi, J. Anal. Appl. Pyrolysis **97**, 55–61 (2012)
11. B. Aslibeiki, G. Varvaro, D. Peddis, P. Kameli, J. Magn. Magn. Mater. **422**, 7–12 (2017)
12. S.A.V. Prasad, M. Deepty, P.N. Ramesh, G. Prasad, K. Srinivasa Rao, Ch. Srinivas, K. VijayaBabu, E. Ranjith Kumar, N. KrishaMohan, D.L. Sastry, Ceram. Inter. 44 (9) 10517 – 10524 (2018)
13. R. Bomila, S. Srinivasan, A. Venkatesan, B. Bharath, K. Perinbam, Mater. Res. Innov **22**, 379–386 (2018)
14. N. Madubuonu, S.O. Aisida, I. Ahmad, S. Botha, T. Zhao, M. Maaza, F.I. Ezema, Bio-inspired iron oxide nanoparticles using Psidium guajava aqueous extract for antibacterial activity. Appl. Phys. A **126**, 72 (2020)